DOI: 10.1002/chem.200800726

Designed Folding of Pseudopeptides: The Transformation of a Configurationally Driven Preorganization into a Stereoselective Multicomponent Macrocyclization Reaction

Ignacio Alfonso,*[a] Michael Bolte,[b] Miriam Bru,[c] M. Isabel Burguete,[c] and Santiago V. Luis*[c]

Abstract: The efficient synthesis of large-ring pseudopeptidic macrocycles through a multicomponent [2+2] reductive amination reaction is described. The reaction was entirely governed by the structural information contained in the corresponding open-chain pseudopeptidic bis(amidoamine) precursors, which have a rigid (*R*,*R*)-cyclohexane-1,2-diamine moiety. A remarkable match/mismatch relationship between the configurations of the chiral centers of the cyclic diamine and those of the peptidic frame was observed. The macrocyclic tetraimine intermediates have been studied in detail by NMR spectroscopy, circular dichroism (CD), and molecular modeling, and the results support the appropriate preorganization induced by the match combination of the chiral centers. We have also synthesized the corresponding open-chain bis(imine) model compounds. The structural studies (NMR spectroscopy, CD, modeling) of these systems showed an intrinsically lower reactivity of the mismatch combination, even when the product of the reaction was acyclic. In addition, a synergistic effect between the two chiral substructures for the correct folding of the molecules was observed. Finally, X-ray analysis of the HCl salt of one of the macrocycles showed an interesting pattern; the macrocyclic rings stack in columnar aggregates leaving large interstitial channels filled with water-solvated chloride anions.

Keywords: conformation analysis · foldamers · macrocycles · peptide-like structures · preorganization

Introduction

Amino acid containing macrocycles[1] are important molecules due to their interesting applications in molecular recognition,[2] biomedicine,[3] and materials science.[4] However, in most cases, their synthesis is hampered by the macrocyclization step, which usually requires high dilution techniques, sophisticated protecting groups, or tedious purification steps.[5] One possible way to improve that process is the conformational preorganization of the linear precursors.[6] However, for the de novo design of a conformation leading to the intended macrocyclic ring, detailed knowledge of the structural variables for the correct folding of the open-chain precursors is mandatory. Therefore, the concept of programmed folding arises as a key to the macrocyclization process.[7] In nature, the structural information implemented within a given sequence leads, under certain environmental conditions, to a functional three-dimensional structure.[8] This is often achieved by the homochirality of the monomers that form the corresponding functional biopolymers.[9] Thus, fundamental information is provided by the geometri-

[a] Dr. I. Alfonso
Departamento de Química Orgánica Biológica
Instituto de Investigaciones Químicas y Ambientales de Barcelona
Consejo Superior de Investigaciones Científicas (IIQAB-CSIC)
Jordi Girona, 18-26, E-08034, Barcelona (Spain)
Fax: (+34) 932-045-904
E-mail: iarqob@iiqab.csic.es

[b] Dr. M. Bolte
Institut für Anorganische Chemie
J. W. Goethe-Universität Frankfurt
Max-von-Laue-Str. 7, 60438, Frankfurt/Main (Germany)

[c] M. Bru, Dr. M. I. Burguete, Prof. Dr. S. V. Luis
Departamento de Química Inorgánica y Orgánica
UAMOA, Universidad Jaume I/CSIC, Campus del Riu Sec
Avenida Sos Baynat, s/n, E-12071, Castellón (Spain)
Fax: (+34) 964-728-214
E-mail: luiss@qio.uji.es

Supporting information for this article is available on the WWW under http://dx.doi.org/10.1002/chem.200800726.

cal parameters obtained by the correct combination of configurations of the corresponding chiral centers, which is expressed when the chiral components are assembled into a larger structure.[10] During the last decade, many chemists have been fascinated by synthetic molecules that have been designed with a preferred conformation in solution, commonly called foldamers.[11] Moreover, some research groups have exploited the potential of structurally designed folding for organic synthesis, especially in the macrocyclic field.[12] For the efficient formation of large rings, the reactive centers must be in a well-defined spatial disposition, namely preorganized in the corresponding cyclic conformation. Therefore, the geometrical parameters of the linear precursors must be carefully tuned for the correct folding, exactly as in nature. To obtain that preorganization, very intelligent approaches have been employed and include geometrical restrictions,[13] intramolecular hydrogen bonding,[14] solvophobic interactions,[15] and π-stacking contacts.[16] However, reports concerning the correlation between different combinations of configurations of the chiral centers and designed folding leading to an intended reactivity are scarce.[17]

On the other hand, we have previously synthesized new pseudopeptidic macrocycles by taking advantage of the U-turn preorganization of this family of compounds in aprotic polar solvents.[18] Some of these systems displayed interesting properties as organogelators,[19] molecular receptors,[20] chemosensors,[21] or molecular devices.[22] Within this research project, we envisioned the preparation of larger structures to expand the possibilities for the generation of a family of compounds by increasing the size and complexity of the substrates. With this in mind, the reductive amination reaction arose as an interesting alternative because imine bonds are rigid and conformationally predictable scaffolds that are very useful for the construction of macrocycles.[23] With this aim, the preorganization of the linear precursor is advisable to obtain acceptable final yields of the macrocyclization product as well as to avoid oligomerization side-products. Accordingly, we recently reported the use of anion templates to promote preorganization for the selective [2+2] cyclization reaction.[24] This conformational trend can alternatively be controlled by the appropriate redesign of linear precursors. Herein we report a detailed structural study of the configurationally driven preorganization of the linear precursors for a highly efficient multicomponent macrocyclization process that leads to new amino acid containing large macrocycles.

Results and Discussion

Design of the macrocyclization reaction: With the aim of preparing large macrocyclic structures, we initially designed a [2+2] reductive amination reaction (Scheme 1) between a pseudopeptidic bis(amidoamine) (**1a**–**i**)[25] and a rigid planar aromatic dialdehyde (**2a**,**b**). However, reactions performed with the flexible derivatives (**1a**,**b**, entries 1 and 2 in Table 1) led to a very complicated mixture of open-chain oligomers with the corresponding [2+2] macrocycles detected by ESIMS only as minor products. These results indicated that the ethylenediamide moiety is too flexible in MeOH to preorganize the system into a macrocycle-producing folded conformation.

After some preliminary molecular modeling, we decided to prepare the corresponding derivatives with a cyclohexane-1,2-diamine moiety, which was selected to favor a rigid and well-defined spatial disposition of the bis(amidoamine) fragment. Chiral cyclohexane-1,2-diamine has previously been used as a scaffold for cyclization processes. Its chairlike conformation, with the C–N bonds forming angles of 60°, has served as an excellent scaffold for the construction of large conformationally restricted macrocycles and pincers. Thus, this diamine can undergo either [2+2] or [3+3] cyclocondensation reactions,[26] generate a dynamic covalent system,[27] or induce important constraints when forming part of a longer open-chain molecule.[28] In our pseudopeptidic molecules, the cyclohexane frame induces a turn conformation in the linear precursors, which favors the [2+2] cyclization process. Satisfyingly, the macrocyclization reaction proceeded smoothly with these redesigned systems. Thus, aldehyde–amine condensation between **1c** and terephthalde-

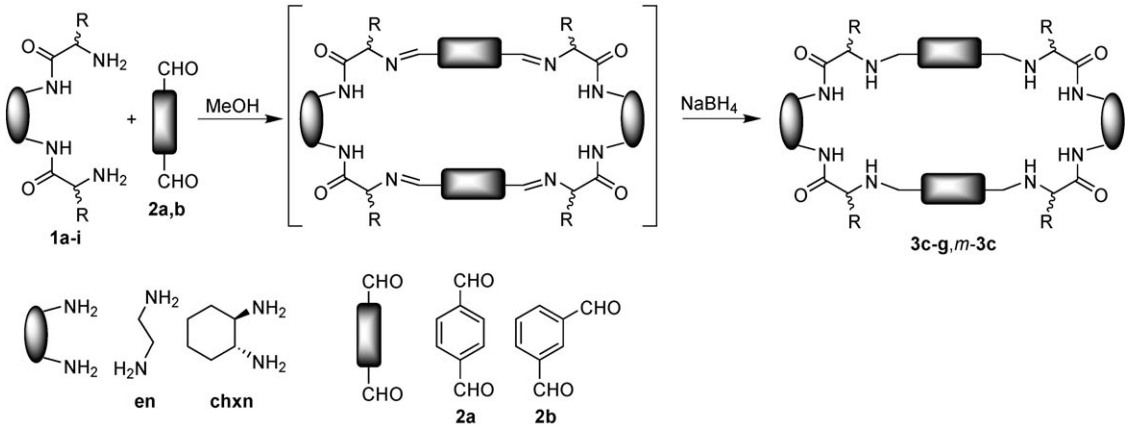

Scheme 1.

Table 1. Results of the multicomponent reductive amination synthesis of pseudopeptidic macrocycles.

	Substrate	Diamine	R (C-α conf.)	Dialdehyde	Product	Yield[a] [%]
1	**1a**	en	*i*Pr (*S*)	**2a**	**3a**	–[b]
2	**1b**	en	CH_2Ph (*S*)	**2a**	**3b**	–[b]
3	**1c**	(*R*,*R*)-chxn	*i*Pr (*S*)	**2a**	**3c**	67
4	**1d**	(*R*,*R*)-chxn	CH_2Ph (*S*)	**2a**	**3d**	55
5	**1c**	(*R*,*R*)-chxn	*i*Pr (*S*)	**2b**	***m*-3c**	35
6	**1e**	(*R*,*R*)-chxn	iBu (*S*)	**2a**	**3e**	58
7	**1f**	(*R*,*R*)-chxn	sec-Bu (*S*)	**2a**	**3f**	41
8	**1g**	(*R*,*R*)-chxn	$(CH_2)_2CONHTr$ (*S*)	**2a**	**3g**	17[c]
9	**1h**	(*R*,*R*)-chxn	*i*Pr (*R*)	**2a**	**3h**	–[b]
10	**1i**	(*R*,*R*)-chxn	CH_2Ph (*R*)	**2a**	**3i**	–[b]

[a] Isolated yield after chromatographic purification. [b] Yield not determined because a complicated mixture of compounds was obtained, as shown by both ESIMS and TLC. [c] Non-optimized yield due to the insolubility of the final compound **3g**.

hyde (**2a**; MeOH, RT, 20 h) led to the macrocyclic tetraimine, which was reduced in situ with sodium borohydride to the corresponding macrocyclic tetraamine **3c** (R = *i*Pr) in a very good overall yield (entry 3, Table 1). To check the generality of the procedure, we changed other fragments of the cyclic structure in a modular way (Table 1). All the final compounds were fully characterized by NMR spectroscopy and mass spectrometry (see the Supporting Information). Owing to the D_2 averaged symmetry of the final macrocycle and to the broadness of the signals in the NMR spectra for most of the derivatives, the accurate ESI-TOF mass spectra were especially illustrative, as unambiguous proof, of the [2+2] macrocyclic structure. In addition, we were able to obtain suitable crystals for X-ray diffraction analysis of one derivative, **3d** (R = Bn, see below). Comparison of the data gathered in Table 1 shows that the reaction can be performed with amino acid precursors with different aliphatic or aromatic side-chains and give comparable final yields (Table 1, entries 4, 6, and 7). The use of the *meta*-dialdehyde (**2b**) instead of the *para* derivative decreased the isolated yield, the rest of the material was recovered as the starting compounds or as open-chain oligomers (Table 1, entry 5). This result suggests that the geometrical disposition around the flat and rigid aromatic spacer is also important, most likely as a consequence of the higher symmetry of the *para*-compared with the *meta*-substituted aromatic dialdehyde. An example with hydrogen-bonding side-chains was also obtained (derived from glutamine, entry 8 in Table 1), although only in moderate (nonoptimized) yield. However, note that the isolation of the final compound (**3g**) was greatly hampered by its very low solubility in most organic solvents.

We also decided to study the effect of different combinations of chiral centers of the linear pseudopeptidic bis(amidoamine) in this macrocyclization reaction. Thus, compounds **1h**,**i** with an *R*,*R* configuration in the cyclohexane moiety, but a D configuration in the amino acid α-carbon atom, were prepared and assayed. Very interestingly for this combination of stereocenters, the reaction led to a mixture of compounds as detected by ^{1}H NMR spectroscopy, TLC, and ESIMS, the major ones corresponding to the starting material (Table 1, entries 9 and 10). This means that there is a cooperative relationship between the chiral centers of the linear molecules, which plays a fundamental role in the macrocyclization reaction. Thus, we obtained a positive (match) combination with (*R*,*R*)-cyclohexane and L-amino acids and, correspondingly, a negative (mismatch) combination with D-amino acids. Therefore, the macrocyclization reaction occurred with a high diastereoselectivity. Because we found these results quite intriguing, we decided to perform an in-depth study of the mechanism of the reaction by characterizing the corresponding tetraimine intermediates.

Structural studies of the macrocyclic tetraimine intermediates: To obtain more precise information about the course of the reaction, we followed (^{1}H NMR, 500 MHz, CD_3OD, 303 K) the formation of the tetraimine intermediate precursor for **3c** (see the Supporting Information). The reaction started just a few minutes after mixing **1c** and **2a**. This was indicated by the gradual disappearance of the aldehyde C*H*O signals ($\delta = 9.99$–10.11 ppm) and the growing of imino methyne signals ($\delta = 8.07$–8.34 ppm). In the first stage of the reaction, a complicated group of signals was formed that simplified after 24 h. At that point, a major compound (ca. 70% from integration of the signals) was obtained with a highly symmetrical geometry, as shown by both its ^{1}H and ^{13}C NMR signals (see the Supporting Information for gCOSY, TOCSY, and ^{1}H–^{13}C gHSQC spectra). This major imine compound exhibited one singlet for the aromatic protons, which can be explained either by a fast rotation of the aromatic ring with respect to the macrocyclic main plane or by a D_2 symmetrical conformation in solution. With regard to the relative disposition between imine bonds, they must all adopt the same *S-trans* configuration or again there must be a fast equilibrium between the *S-cis* and *S-trans* configurations in the NMR timescale to render the observed D_2 symmetry. The presence of other minor imino signals (overall accounting for around an additional 25%) and the fact that no other cyclic compounds were isolated after reduction suggest that these minor nonsymmetrical imino groups arise from the presence of different relative dispositions of the C=N double bonds and support the assumption that the major compound is an all-*S-trans* isomer. All of these imino signals also showed strong NOE effects with the α-H protons of the peptidomimetic moiety (see the Supporting Information for 2D NOESY spectra), which supports the connectivity between the two substructures and a *syn* disposition of these protons in the major species, as depicted in Scheme 2.

Despite this, the strong geometrical preference for the system to form the D_2 symmetrical cyclic structure is highly

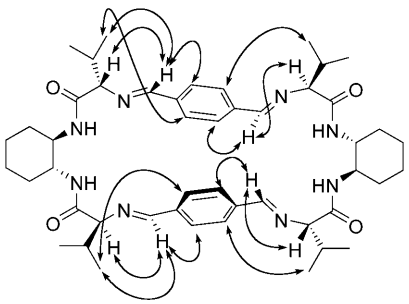

Scheme 2. Observed NOEs for the macrocyclic tetraimine intermediate obtained from the condensation reaction between **1c** and **2a**.

remarkable. The composition of this mixture does not change over a long period of time (>8 weeks) or by heating the sample up to 60 °C, which supports the suggestion that it is an equilibrium mixture under thermodynamic control. Note also that performing the same experiment with **1h** (derived from D-valine) instead of **1c** (derived from L-valine) led to a very complicated group of signals in the ^{1}H NMR spectrum and to the incomplete consumption of dialdehyde **2a** even over very long reaction times (>3 d, see the Supporting Information). This is also solid proof for the match/mismatch effect of the configurations of the chiral centers.

The formation of the tetraimine intermediate was also studied by electronic circular dichroism (CD).[29] The CD spectrum of a mixture of **1c** and **2a** after 24 h of reaction time clearly showed a bisigned (−,+) curve (black line in Figure 1) with a minimum at 296 nm ($\Delta\varepsilon = -110\ cm^2\,mmol^{-1}$) and a maximum at 269 nm ($\Delta\varepsilon = 132\ cm^2\,mmol^{-1}$). The CD bisigned signal passes through zero at 280 nm, which is the λ_{max} ($\varepsilon = 59600\ M^{-1}cm^{-1}$) of the UV absorbance (Figure 1). This UV band can be assigned to π–π* transitions of the aromatic diimine.[30] The CD spectrum unambiguously implies a negative split-Cotton effect, which allowed us to determine the disposition of the chromophores in solution because the dipole moment associated with the π–π* transition in this chromophore is known.[30] The magnitude of the amplitude is in agreement with a highly chiral and ordered structure with the corresponding chromophores, namely the aromatic diimines, in close proximity to one another. In addition, for an appropriate comparison, we prepared the corresponding (*R*,*R*)-cyclohexane-1,2-bis(benzylimine) [(*R*,*R*)-**4**] and its CD spectrum was measured under the same conditions (dotted line in Figure 1). This compound showed a very similar split-Cotton effect of negative sign (−,+), although at a shorter wavelength due to less conjugation in the chromophores. All these data imply that the chirality and the geometrical disposition of the (*R*,*R*)-cyclohexane-1,2-diamine have been efficiently transferred throughout the whole system of the macrocyclic tetraimine formed by the reaction between **1c** and **2a**. Even more interestingly, the corresponding experiment with the mismatch combination of stereocenters (**1h**+**2a**) gave a less intense CD spectrum (grey line in Figure 1) with no sign of exciton-coupling. These results highlight the importance of the configurationally driven preorganization of precursors for the correct folding of the system.

We also performed some molecular modeling studies to visualize these effects. Thus, Monte Carlo conformational searches with MMFF minimizations were performed for the proposed macrocyclic tetraimines derived from either **1c** (match) or **1h** (mismatch) pseudopeptides (Figure 2). Interestingly, the cyclic compound with the match relationship rendered a global minimum with a structure in very good agreement with the experimental data (Figure 2A). It shows an average D_2 symmetry with interatomic distances compatible with the observed NOE contacts. The cyclohexanes are in a perfect chair conformation with the substituents in equatorial positions. The structure presents an all-*S*-*trans* relative disposition of the imine bonds and a flat conformation for the aro-

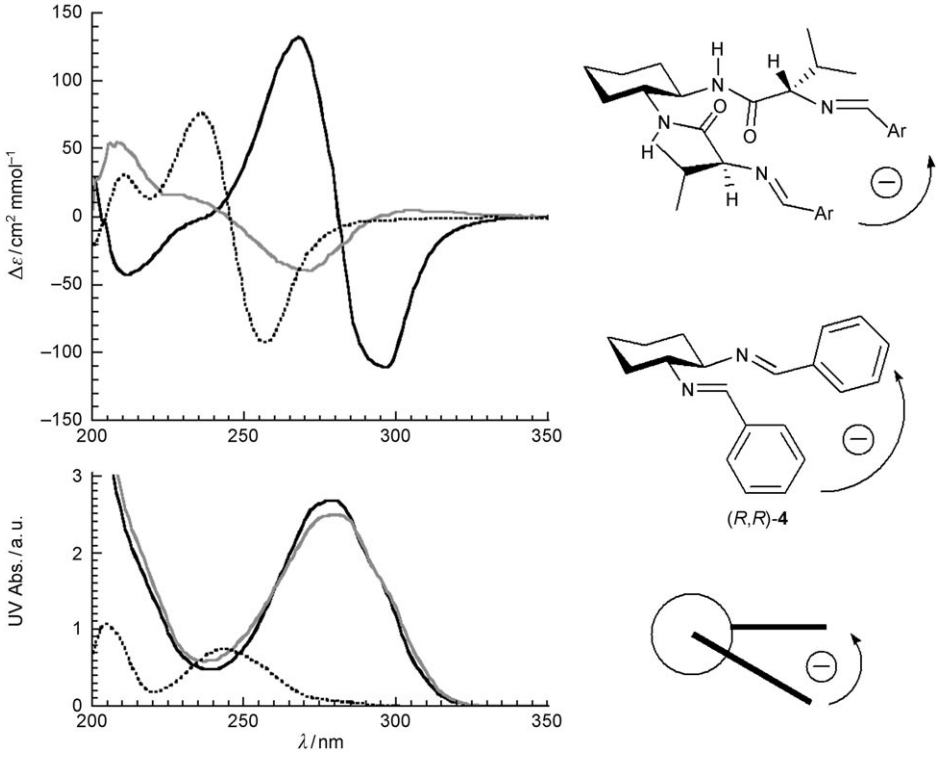

Figure 1. CD (top) and UV (bottom) spectra of the reactions between **1c**+**2a** (black), **1h**+**2a** (grey), and (*R*,*R*)-**4** (dotted).

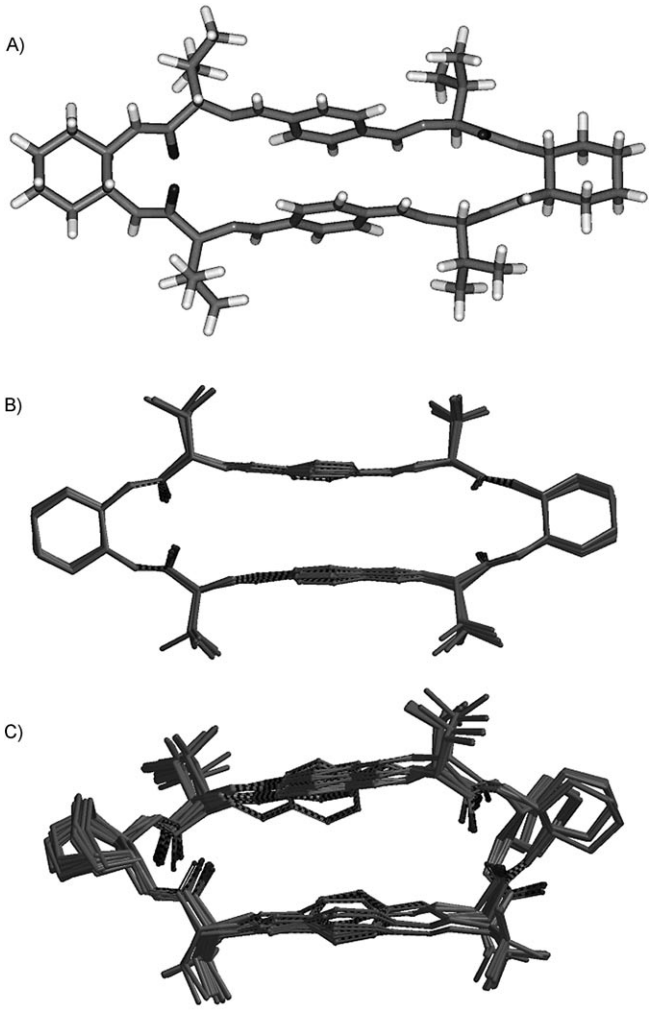

Figure 2. A) Minimized geometry of the macrocyclic tetraimine that leads to **3c**. B,C) Superposition of the energetically accessible (1% from a Boltzmann distribution) local minima (Monte Carlo searches with MMFF minimizations) of the macrocyclic tetraimines obtained from **1c** (B, match) or **1h** (C, mismatch). Hydrogen atoms have been omitted for clarity in B and C.

matic diimine groups, which maximizes the conjugation of the system. The isopropyl side-chains are set in equatorial positions, pointing away from the macrocyclic structure. In addition, superposition of the energetically accessible local minima (Figure 2B) showed a rigid averaged oval shape with slight changes in the dispositions of the side-chains but retaining the conformation of the macrocyclic backbone. However, the same calculations performed with the hypothetical macrocycle derived from **1h** with mismatch configurations rendered very different results. The macrocycle showed an averaged distorted geometry with a large number of structurally different accessible minima (Figure 2C). Most of them showed the cyclohexane moiety in a highly strained boat conformation and/or the *i*Pr group in a pseudoaxial position, which must be energetically demanding. In fact, the global minimum of this system (**1h**) is much less stable (6.58 kcal mol^{-1}) than the diastereomer derived from **1c**. All these theoretical results also indicate that the mismatch configurations do not favor the formation of the macrocycle, as observed experimentally. In addition, as the system is under thermodynamic control, these theoretical calculations must reflect a reliable picture of the process.

Open-chain model systems: Taking into account the match/mismatch effect observed for the macrocyclization reaction, we wondered if that behavior is controlled by the structural differences of the pseudopeptidic repeating units. In other words, whether the different reactivity depends completely on the formation of the macrocycle or whether it is inherent to the pseudopeptidic moiety. Thus, we prepared four different open-chain model compounds (**5a–d**) with similar pseudopeptide–imine linkages. We synthesized both the match (**5a**) and mismatch (**5b**) combinations of the cyclohexane

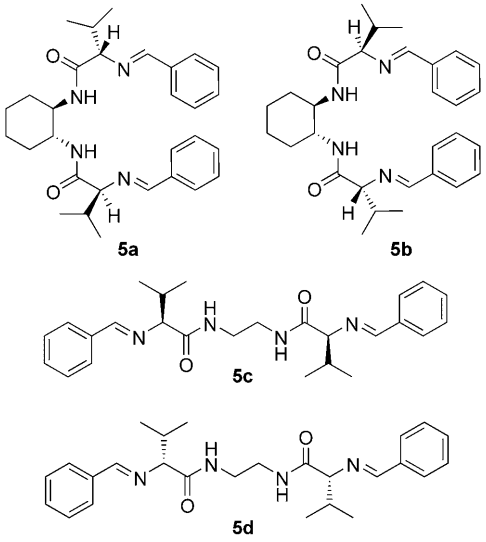

derivatives, whereas for the flexible ethylene compounds, we prepared two enantiomers (**5c**,**d**). The compounds were synthesized by a simple condensation reaction between the corresponding bis(amidoamine) and benzaldehyde in methanol. Rather interestingly, the rate of formation of the imine bond (estimated by ^{1}H NMR spectroscopy) was much lower for the mismatch combination (**5b**) than for the match diastereomer (**5a**). For instance, the reaction showed 98% imine conversion for **5a** after 23 h (10 mM, CD_3OD, 303 K), but a 78% conversion for **5b** for the same reaction time. This last derivative required 75 h to achieve 93% imine conversion by NMR spectroscopy. Accordingly, there is a difference in the reactivity of the initial diastereomeric bis(amidoamine) pseudopeptides **1c** and **1h**. Thus the difference in the macrocyclization is not exclusively due to differences in strain in the final cyclic structure, as can be observed even in condensation reactions that lead to open-chain imines.

The different reactivities observed for **1c** and **1h**, which lead to **5a** and **5b**, respectively, can be rationalized by considering the geometry of the possible conformations of the

two compounds **1c** and **1h** in solution (Scheme 3). By assuming diequatorial positioning of the amide groups on the cyclohexane moiety and a *trans* disposition of the peptidic

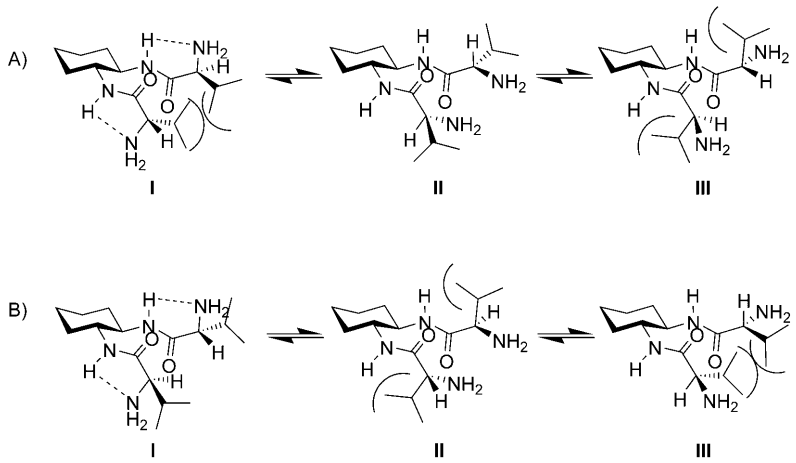

Scheme 3. Proposed conformational equilibrium for A) **1c** and B) **1h**.

bonds, three different rotamers of the carbonyl–Cα bond can be proposed (conformers **I–III** in Scheme 3). According to the ^{1}H and ^{13}C NMR spectroscopy data, only C_2 symmetrical conformations will be considered, although other nonsymmetrical geometries in dynamic equilibrium could also be present in solution. The stability, and therefore, the population of these species depend on the stabilizing/destabilizing interactions found in each case. For instance, conformer **I** in compound **1c** would allow amide–amine N−H···N hydrogen-bonding interactions, thereby forming intramolecular five-membered rings (Scheme 3a). These interactions have previously been found for related systems both in solution[18,22] and in the solid state.[18] However, this conformation (**I**) would present a large steric hindrance between the isopropyl groups. On the other hand, in conformer **III** of the same compound the amide N−H and *i*Pr groups would be eclipsed, which would result in a destabilizing interaction. Therefore, in polar protic solvents, conformer **II** is expected to be slightly favored for **1c** as the steric hindrance between the *i*Pr groups would be diminished because they would be in pseudoequatorial positions and far away from each other.

In the case of compound **1h** (Scheme 3b), the scenario would be much clearer because two of the rotamers (**II** and **III**) show steric hindrance arising from the *i*Pr groups, whereas in conformer **I** the two *i*Pr groups would be pseudoequatorial and would also exhibit the proposed amide–amine hydrogen-bonding stabilizing interactions. Therefore, conformer **I** should be the most populated for **1h**. By comparing both structures (**II** for **1c** versus **I** for **1h**) one can predict that the amino nitrogen atoms in **1h-I** must be less nucleophilic than those in **1c-II** because their lone-pair electrons are involved in intramolecular hydrogen bonds.[31] Although MeOH would be able to break these hydrogen-bonding interactions, a clear difference in reactivity was observed, which can be ascribed to these structural differences. Monte Carlo studies of these systems showed that the type **I** conformers would be the most favorable for both diastereomers. This could be due to an overestimation of the hydrogen-bonding stabilization within the force-field calculations (even by using polar solvents such as water in the calculations). However, the corresponding minimum for **1h** is more stable (2.16 kcal mol^{-1}) than that of **1c**, probably due to the above-mentioned steric hindrance in **1c-I**. These computational results are in line with our initial hypothesis.

Once the model compounds (**5a–d**) had been prepared, we studied their conformations in solution. First of all their ^{1}H NMR spectra showed important differences, especially in the imine-linkage region. The ^{1}H chemical shifts of **5a** are very similar to those of the flexible ethylene derivatives **5c**,**d** (Figure 3, Table 2, entries 1 and 6). However, compound **5b** showed a more complex group of signals that indicated the presence of at least four different imine groups. Integration of the different ^{1}H NMR signals showed the species to be present in a ratio of 80:14:3:2; some representative chemical shifts are gathered in Table 2. The minor ones (overall accounting for 19%) showed chemical shifts very similar to those of **5a,c,d**. However, for the major species (80%), the

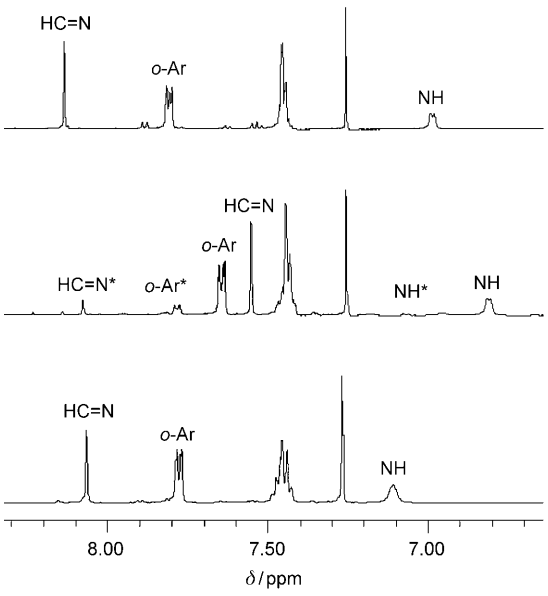

Figure 3. Selected region of the ^{1}H NMR spectra of **5a** (upper trace), **5b** (middle trace), and **5c**,**d** (lower trace). Signals corresponding to the minor species in **5b** are shown with asterisks.

Table 2. Chemical shifts of selected ^{1}H NMR signals of **5a–d**.

	Compound	Isomer [%]	*HC*=N	*o*-ArH	α-H	Amide NH
1	**5a**	n.a.	8.14	7.81	3.57	6.99
2	**5b**	80	7.56	7.65	3.15	6.82
3	**5b**	14	8.08	7.79	3.54	6.96
4	**5b**	3	8.15	7.84	3.60	7.19
5	**5b**	2	8.24	7.96	3.57	7.19
6	**5c**,**d**	n.a.	8.07	7.77	3.58	7.11

protons surrounding the imine linkage shift upfield with respect to the corresponding signals of **5a** (Table 2, entries 1 and 2). This shielding can only be explained by the presence of a conformation in which the aromatic ring of one benzylimine group is above the proton nuclei (aromatic imine and α-carbon atom) of the other equivalent arm in a C–H···π disposition.

With the aim of explaining these experimental differences, we performed some molecular modeling calculations on **5a**,**b** (Figure 4). Monte Carlo searches on these systems supported the data obtained by NMR spectroscopy. Thus, **5a** behaved slightly more flexible in solution, which accounts for the chemical shifts being similar to those of **5c**,**d**. However, **5b** seemed to be more conformationally constrained; in the accessible minima the protons of one aromatic imine group (namely, HC=N, α-H, and *o*-Ar-H) are above the anisochronic shielding cone of the other aromatic ring (Figure 4). This disposition explains the observed upfield shifts for **5b**. Although the computed geometries are not actually symmetrical, a dynamic equilibrium on the NMR timescale would produce an averaged C_2 symmetry, as experimentally observed.

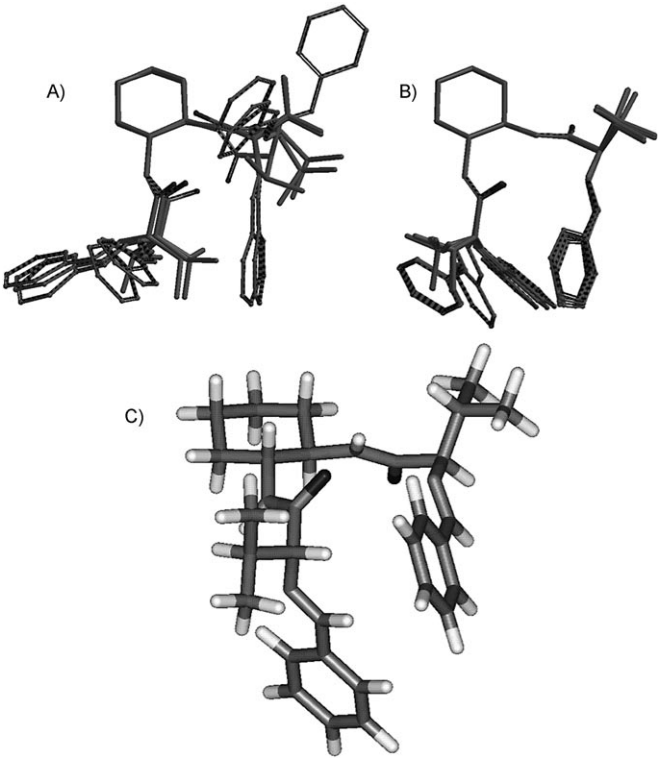

Figure 4. Superposition of the energetically accessible local minima for A) **5a** and B) **5b**. The global minimum for **5b** is also shown (C) in a different perspective to highlight the disposition between the aromatic imines.

We also performed NOESY experiments on **5a**,**b** (see the Supporting Information). For the match diastereomeric combination, strong NOE cross-peaks were observed, in agreement with the presence of a conformation very similar to that proposed for the cyclic tetraimine intermediate (Scheme 4). However, a weaker NOE effect between the amide NH and the *ortho* proton of the aromatic ring suggests the participation of other conformations with the benzylimine group in a pseudoaxial position (Scheme 4). The same experiment performed with **5b** was inconclusive because the observed NOEs were of a much lower intensity than those for **5a** and indicated an imine linkage.

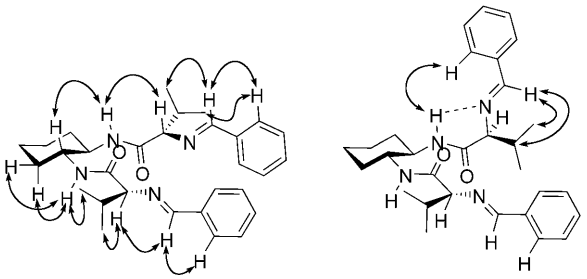

Scheme 4. Observed NOEs for compound **5a**.

As a complementary technique, we also recorded the CD spectra of the model compounds **5a–d** in methanol. The flexible derivative **5c** (Figure 5, black trace) showed a strong CD signal of the type (−,+,−) characterized as follows: $\lambda_{min}=277$ nm, $\Delta\varepsilon=-7.5$ cm^{2}mmol^{-1}; $\lambda_{max}=244$ nm, $\Delta\varepsilon=+20.8$ cm^{2}mmol^{-1}; $\lambda_{min}=215$ nm, $\Delta\varepsilon=-16.0$ cm^{2}mmol^{-1}. As expected, its enantiomer **5d** (Figure 5, grey line) displayed a perfect mirror image (+,−,+) CD spectrum. The UV absorbance at $\lambda_{max}=250$ nm ($\varepsilon=40\,000$ M^{-1}cm^{-1}) can be assigned to the π–π* transitions of aromatic imine chromophores. The absence of a clear exciton-coupling effect prevented the preferred conformation being proposed, but the results obtained for the macrocyclization reaction suggest that these systems are highly flexible in methanol. Therefore, these spectra can be considered as a random coil CD reference.

Some interesting trends were observed in the CD spectra of the cyclohexane derivatives **5a**,**b**. First, for **5b** (Figure 6, grey line), the CD signal shifted to more negative values ($\lambda_{max}=275$ nm, $\Delta\varepsilon=+3.7$ cm^{2}mmol^{-1}; $\lambda_{min}=245$ nm, $\Delta\varepsilon=-26.9$ cm^{2}mmol^{-1}; $\lambda_{max}=220$ nm, $\Delta\varepsilon=+13.7$ cm^{2}mmol^{-1}) relative to the signals of the corresponding flexible reference compound **5d**. Once again, no split-Cotton signal was detected, which suggests that a preorganization suitable for

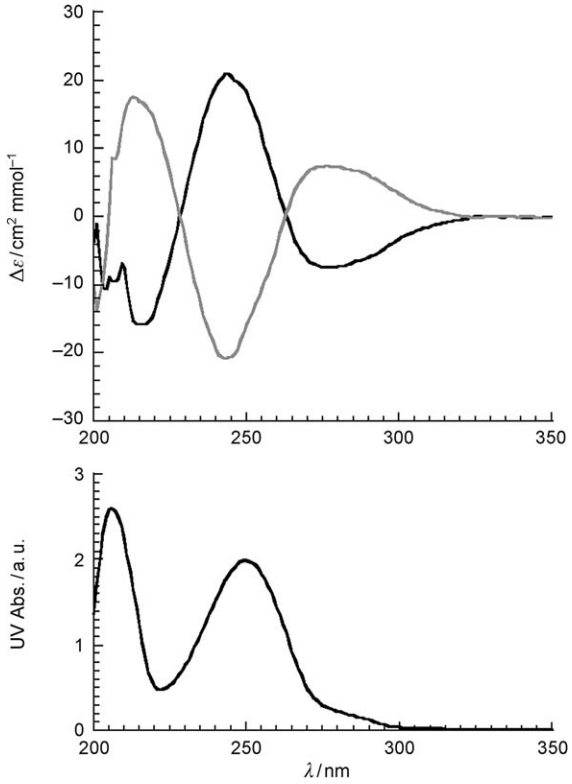

Figure 5. CD (top) and UV (bottom) spectra of **5c** (black) and **5d** (grey).

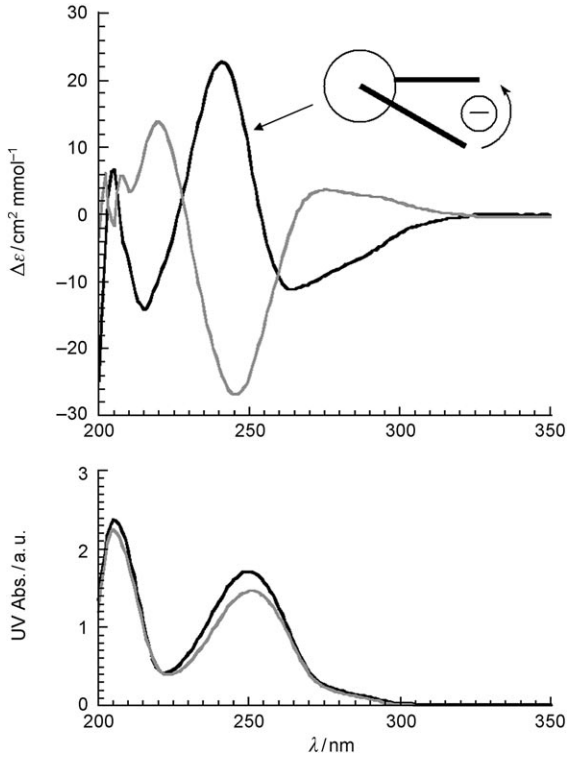

Figure 6. CD (top) and UV (bottom) spectra of **5a** (black) and **5b** (grey).

the macrocyclization process is not present in solution. Fortunately, the CD data for **5a** were much more informative (Figure 6, black line). A comparison of the CD data for **5a** with that for the flexible derivative **5c** shows that the first minimum decreases in intensity ($\lambda_{min}=265$ nm, $\Delta\varepsilon=-11.2\ cm^2\,mmol^{-1}$), the subsequent maximum increases in intensity ($\lambda_{max}=241$ nm, $\Delta\varepsilon=+22.7\ cm^2\,mmol^{-1}$), and the second minimum also increases ($\lambda_{min}=215$ nm, $\Delta\varepsilon=-14.1\ cm^2\,mmol^{-1}$). A slight blueshift of the CD spectrum was observed as a consequence of an incipient exciton-coupling effect. In addition, as the UV absorbance shows a maximum at $\lambda_{max}=250$ nm ($\varepsilon=34\,500\ M^{-1}cm^{-1}$) and the CD passes through zero at $\lambda_{max}=254$ nm, there must be a contribution from bisigned exciton-coupling for the π–π* transition of the aromatic imines. In addition, this split-Cotton effect clearly implies negative chirality.

The negative sign of the split-Cotton effect of the imines in **5a** reflects the effective preorganization induced by the cyclohexane moiety, despite its open-chain nature. This preorganized conformation was observed in the macrocyclic tetraimine and must be the effective driving force for the [2+2] multicomponent cyclization. Moreover, we aimed to determine the contribution of each substructure (pseudopeptide and cyclohexane) in the overall preorganization.[32] To do that, we attempted to deconvolute the CD spectrum of **5a** into the corresponding two reference spectra for both substructures. Accordingly, we utilized **5c** as the reference for the pseudopeptidic contribution and (*R*,*R*)-**4** (Figure 1) as the reference for the cyclohexane framework. Satisfyingly, we were able to reasonably reproduce the CD spectrum of **5a** (Figure 7) as a weighted combination of the two substructures, rendering an approximate contribution of $\Delta\varepsilon_{\mathbf{5a}} \approx 0.86\Delta\varepsilon_{\mathbf{5c}}+0.14\Delta\varepsilon_{(R,R)\text{-}\mathbf{4}}$. In addition, the amplitude of the CD signal is inversely proportional to the square of the distance between the interacting chromophores, and that distance should be shorter for (*R*,*R*)-**4** than for **5a**. Thus, we have used a model subsystem with a stronger CD signature than that possible in **5a**. Consequently, the actual conformational contribution of the cyclohexane moiety must be

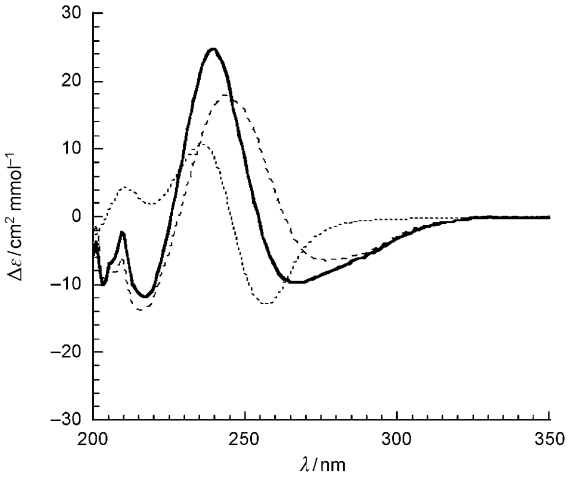

Figure 7. Simulation of the CD spectra of **5a** (black) obtained by the addition of weighted CD spectra of the corresponding substructures: $0.86\Delta\varepsilon_{\mathbf{5c}}$ (dashed) $+0.14\Delta\varepsilon_{(R,R)\text{-}\mathbf{4}}$ (dotted).

larger than that calculated by our approach (14%). Anyway, this remarkable relationship can be understood as a semi-quantitative expression of the match effect of the chiral centers on the conformational preorganization.

Overall, this in-depth structural study of open-chain model compounds has allowed important conclusions to be drawn regarding the match/mismatch effect of the chiral centers. First, the amino nitrogen atoms in **1c** are intrinsically more nucleophilic than those in **1h**. On the other hand, the NMR spectroscopy data suggest that **5a** is slightly more flexible than **5b** because in the latter the close proximity of the aromatic diimines leads to some conformational constrictions. However, despite the higher flexibility of **5a**, its chiral centers enable the compound to adopt a conformation suitable for macrocyclization, as demonstrated by the NOEs and CD results. More interestingly, for **5a**, we have been able to quantify the contribution of each substructure to the averaged conformation in solution. Therefore, we have demonstrated that the positive/negative preorganization for cyclization involves a match/mismatch combination of the two substructures (cyclohexane and peptidic) present in the molecules.

Crystal structure of 3d·4HCl: We were able to obtain crystals of the tetrahydrochloride salt of **3d** suitable for X-ray diffraction analysis. The results are shown in Figures 8 and 9. The nanometer-sized (1.1×2.0 nm) macrocycle adopts a conformation with almost D_2 symmetry, as shown in Figure 8A. The cyclohexane moiety adopts a chair conformation with the amide substituents in equatorial positions. The amide NH groups are *trans* with respect to the methynes of the chiral centers of the cyclohexane rings and *cis* to the α-hydrogen atoms of the peptidic fragments. The benzyl side-chains are in pseudoequatorial positions and point away from the macrocyclic ring. Interestingly, the aromatic rings of the side-chains are folded towards the cyclohexane moieties, thereby forming a hydrophobic core that seems to play an important role in the crystal packing (see below). The amino nitrogen atoms are fully protonated and point out from the macrocycle, thereby minimizing the mutual electrostatic repulsions. The aromatic rings of the backbone phenylene groups are perpendicular to the macrocyclic main plane and very close to each other, which possibly allows π-stacking interactions to be established (interplanar distance ≈3.6–3.7 Å). Overall, the conformation of the pseudopeptidic moiety is in good agreement with that proposed for the precursor tetraimine intermediate. The crystal has four chloride anions per macrocycle. Two of them are above each pseudopeptidic moiety and establish hydrogen-bonding interactions with the amide N*H* and N–CH_2–Ar hydrogen atoms (Figure 8B). These interactions stabilize the stacking of the macrocyclic rings within a columnar supramolecular aggregate (Figure 8C). The other two chloride atoms are outside the macrocyclic cavity.

The packing of the columnar aggregates is also noteworthy. The cores formed by the benzyl side-chains and the cyclohexane rings interpenetrate on two opposite faces of the

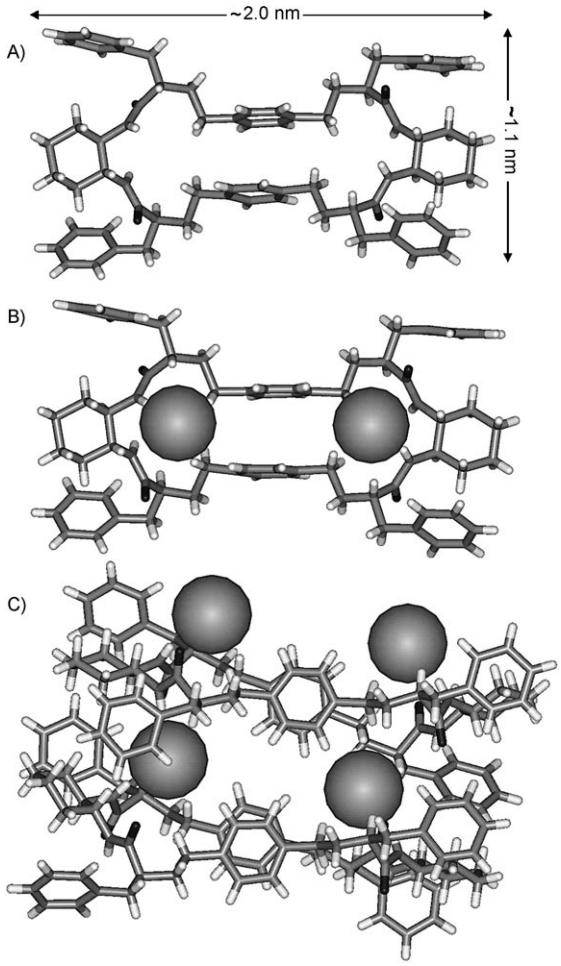

Figure 8. A) Top view of the macrocyclic tetracation alone and B) with two hydrogen-bonded chloride anions. C) Side view of the columnar stacked aggregation assisted by chloride anions (chloride ions are represented in the CPK model).

columns, which leads to tight packing of the columns through aryl–aryl and hydrophobic contacts. The other two faces leave large interstitial channels between the columns (see Figure 9A for the top view of empty channels). These channels have a rhomboid-shaped section with an estimated area of 92.4 Å^2. They are filled with chloride anions and water molecules as the ammonium groups point towards the inner face of the interstitial holes, which makes them highly hydrophilic (see Figure 9B for top view of the filled channels). A longitudinal section of the channel (Figure 9C) shows an interesting pattern with solvated chloride anions along the whole channel. Accordingly, the whole crystal structure can alternatively be described as water-filled chloride channels embedded in a hydrophobic core.

Conclusion

We have developed a multicomponent reductive amination macrocyclization reaction for the synthesis of new amino

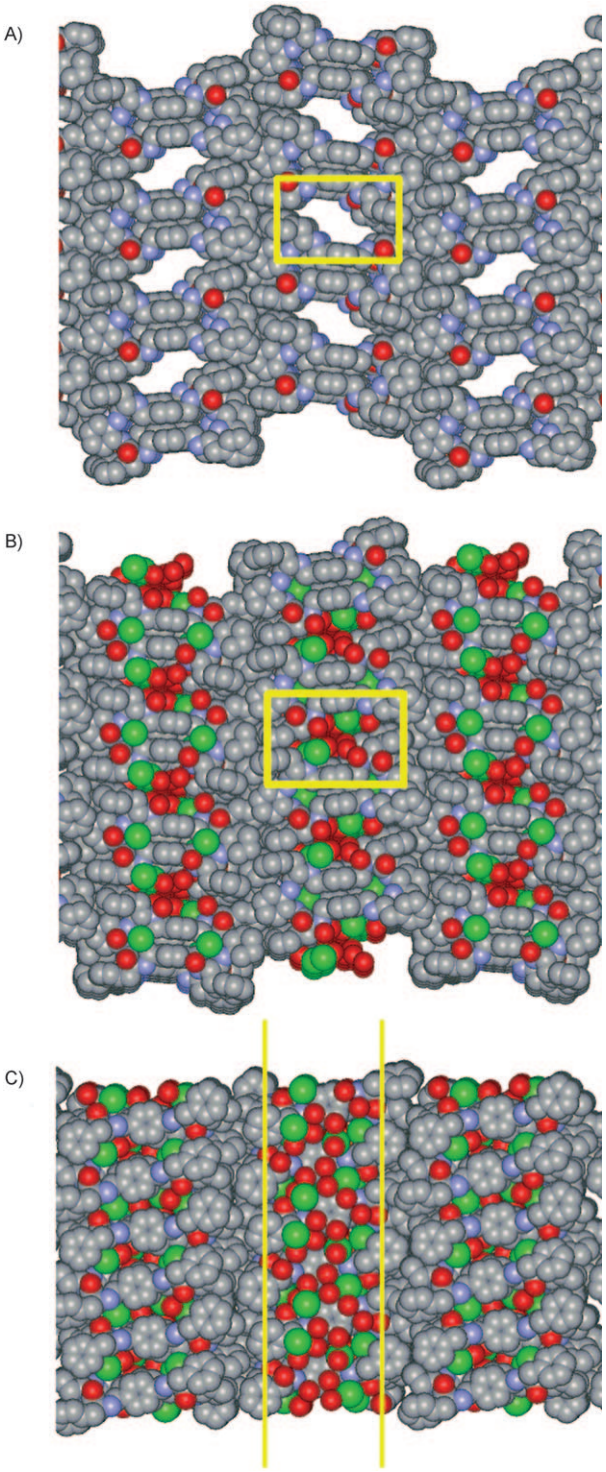

Figure 9. CPK representation of the crystal packing of **3d**·4HCl. Upper view of the interstitial channels A) without and B) with chloride anions and solvent molecules. C) Longitudinal section of the chloride and water filled channels. Hydrogen atoms have been omitted for clarity (carbon: grey; nitrogen: blue; oxygen: red; chloride: green).

acid containing macrocycles. The efficiency of the reaction is strongly dependent on the structural parameters of the open-chain pseudopeptidic bis(amidoamine) linear precursors. Moreover, the macrocyclization process is dominated by a match/mismatch relationship of the relative configuration of the chiral centers in both substructures: the cyclic diamine and peptidic moieties. The correct combination is that with (*R*,*R*)-cylohexane-1,2-diamine and L-amino acids. This effect has clearly been demonstrated by a study of the macrocyclic tetraimine intermediates by different experimental (CD and NMR spectroscopy, including NOEs) and theoretical (Monte Carlo conformational searches) methods.

The match/mismatch effect on the reactivity has been further studied by using the corresponding open-chain model systems. From their detailed structural characterization (NMR spectroscopy, CD, and modeling), some important conclusions can be extracted. First, the mismatch combination of the chiral centers has an intrinsically lower reactivity, even for a reaction leading to open-chain products. In addition, the slightly larger flexibility of the match diastereomer allows it to adopt a folded conformation that leads to macrocyclization. More importantly, the CD spectra of all the model systems clearly indicate the synergistic effect between the two (diamine and peptidic) substructures. For the match combination, this cooperative folding is expressed by a weighted participation of each conformation in the overall folding.

Finally, the crystal structure of the tetrahydrochloride salt of macrocycle **3d** showed very interesting behavior. The nanometric macrocycles stack in a columnar supramolecular structure held together with the help of hydrogen-bonding interactions with two chloride anions. These columnar entities are hydrophobically packed leaving interstitial channels filled with chloride anions and water molecules. This supramolecular crystal packing can be described as an anion channel inside a hydrophobic core. Anion channels are highly important entities both in chemistry[33] and in biology.[34] Our results show the potential of these simple macrocycles for preparing synthetic minimalistic chloride channels.

Experimental Section

General: Reagents were purchased from commercial suppliers (Aldrich, Fluka, or Merck) and were used without further purification. Compounds **1a–i** were prepared following slight variations of previously reported procedures for linear diamines.[18,24] Experimental and spectroscopic details are given in the the Supporting Information.

The NMR experiments were carried out either on a Varian INOVA 500 (500 MHz for ^{1}H and 125 MHz for ^{13}C) or a Varian MERCURY 300 spectrometer (300 MHz for ^{1}H and 75 MHz for ^{13}C). Chemical shifts are reported in ppm using residual nondeuteriated solvent peaks as internal standards. Mass spectra were recorded on a hybrid QTOF I (quadrupole-hexapole-TOF) mass spectrometer with an orthogonal Z-spray/electrospray interface (Micromass, Manchester, UK) or on a Micromass Quattro LC spectrometer equipped with an electrospray ionization source and a triple-quadrupole analyzer. Infrared spectra were recorded on a Perkin-Elmer 2000 FT-IR spectrometer.

CD spectra were recorded with a JASCO J-810 spectropolarimeter at RT. The normalized spectra were obtained by transforming the molar circular dichroic absorption data ($\Delta\varepsilon$, cm^2 mmol^{-1}) using the formula: $\Delta\varepsilon = \theta/(32\,980Cl)$, in which θ is the measured ellipticity (in mdeg), C is the

concentration (in M), and l is the pathlength (in cm). No changes were observed for normalized spectra at different overall concentrations.

Suitable crystals of **3d** for X-ray diffraction were obtained as follows: A small amount of pseudopeptidic macrocycle **3d** (≈3 mg) was dispersed in HPLC-grade methanol (1 mL). Then a small excess of 10% aqueous HCl was added dropwise until complete dissolution. Crystals of **3d**·4HCl were obtained by the very slow (several weeks) evaporation of the solvents. $C_{64}H_{80}N_8O_4{\cdot}4Cl^-{\cdot}8H_2O$; formula weight 1311.29; orthorhombic; space group $P2_12_12_1$; $a=13.0283(15)$, $b=13.0834(10)$, $c=42.757(4)$ Å; $V=7288.1(12)$ Å^3; $Z=4$; colorless block-shaped crystals; STOE-IPDS-II two-circle diffractometer; $T=173$ K; $Mo_{K\alpha}$ radiation; 2θ range = 3.26–51.36°; 26237 reflections collected; 12668 independent reflections ($R_{int}=0.1586$); empirical absorption correction[35] (MULABS); structure solution with SHELXD, refinement on F^2 with SHELXL-97,[36] $R_1[I>2\sigma(I)]=0.1215$, GOF = 0.858. The absolute configuration was determined: Flack x parameter = −0.06(18). All non-hydrogen atoms were refined anisotropically. Hydrogen atoms were generated according to the stereochemistry and refined by using a riding model. CCDC-682038 contains the supplementary crystallographic data for this paper. These data can be obtained free of charge from The Cambridge Crystallographic Data Centre via www.ccdc.cam.ac.uk/data_request/cif.

Molecular modeling: All the theoretical calculations were performed using Spartan '06 program.[37] The optimized geometries for the corresponding minima were obtained as follows: A stochastic conformational search was applied (Monte Carlo search followed by MMFF force-field minimization) without restrictions to each compound. More than 100 conformers were obtained in this way (with a cut off of ca. 10 kcal mol^{-1}). The structures obtained were ordered by their energies and analyzed. The Boltzmann distributions of the corresponding conformers were calculated at 298.15 K and the superposition of the energetically accessible local minima were carried out by using the same software package.

General procedure for the macrocyclization reaction—synthesis of compound 3c: Compound **1c** (160 mg, 0.512 mmol) was dissolved in degassed CH_3OH (5 mL) and the solution was placed inside a flask under nitrogen. Terephthaldehyde (70 mg, 0.512 mmol) was dissolved in degassed CH_3OH (3 mL) and this solution was added to the solution of **1c** and then, CH_3OH (2.5 mL) was added to give a final volume of 10.5 mL (a final concentration of 0.05 M for each reagent). The mixture was stirred overnight. After 20 h a large excess of $NaBH_4$ (158 mg, 4.096 mmol) was carefully added and the mixture was allowed to react for 24 h before being hydrolyzed (concd HCl, to acidity) and evaporated to dryness. The residue thus obtained was dissolved in water and basified with 1 N NaOH. The product was extracted with $CHCl_3$. The combined organic layers were dried ($MgSO_4$) and the solvents were evaporated in a vacuum. The product was purified by silica flash chromatography using CH_2Cl_2 as the eluent while slowly increasing the polarity with MeOH; several drops of NH_3 were added to the mobile phase to improve the extraction of the product. The product was characterized as the corresponding HCl salt, prepared by addition of concd HCl to a methanolic solution of the free amine. Yield: 67%; pale-yellow solid; m.p. >230°C (decomp); $[\alpha]_D^{20}=+11.59$ ($c=0.92$ in CH_3OH); ^{1}H NMR (CD_3OD, 500 MHz): $\delta=1.06$ (d, $J=6.8$ Hz, 12H), 1.12 (d, $J=6.7$ Hz, 12H), 1.30–1.41 (m, 8H), 1,77 (brs, 4H), 2.13 (d, $J=11.4$ Hz, 4H), 2.29–2.36 (m, 4H), 3.83 (d, $J=4.9$ Hz, 4H), 3.88 (brs, 4H), 4.14 (ABq, $\delta_A=4.10$, $\delta_B=4.18$ ppm, $|J_{AB}|=13.3$ Hz, 8H), 7.60 (s, 8H), 8.52 ppm (brs, 4H, exchangeable with solvent); ^{13}C NMR (D_2O, 75 MHz, 90°C): $\delta=18.1$, 19.3, 25.5, 30.8, 33.9, 50.8, 53.8, 66.2, 132.4, 133.2, 167.7 ppm; IR (KBr): $\tilde{\nu}=3399$, 3210, 3055, 2967, 2937, 2856, 1665, 1551 cm^{-1}; MS (ESI-TOF): m/z (%): 415.5 (100) $[M+2H]^{2+}$.

Compound 3d: This compound was obtained as described above starting from **1d** and terephthaldehyde, and was characterized as the corresponding HCl salt. Yield: 55%; pale-yellow solid; m.p. 230°C (decomp); $[\alpha]_D^{20}=+26.79$ ($c=0.89$ in CH_3OH); ^{1}H NMR (CD_3OD, 500 MHz): $\delta=0.57$ (brd, $J=12.9$ Hz, 2H), 0.68 (brs, 2H), 1.00–1.07 (m, 4H), 1.28–1.32 (m, 4H), 1.48 (brd, $J=8.8$ Hz, 4H) 3.02 (t, $J=11.8$ Hz, 4H), 3.45 (dd, $J_1=13.1$, $J_2=5.0$ Hz, 4H), 4.03 (dd, $J_1=10.5$, $J_2=5.1$ Hz, 2H), 4.20 (ABq, $\delta_A=4.15$, $\delta_B=4.26$ ppm, $|J_{AB}|=12.9$ Hz, 8H), 7.25–7.35 (m, 20H), 7.69 ppm (s, 8H); ^{13}C NMR (CD_3OD, 125 MHz): $\delta=25.2$, 33.0, 36.8, 50.3, 53.7, 63.4, 128.8, 130.0, 130.8, 132.3, 133.5, 135.4, 168.5 ppm; IR (KBr): $\tilde{\nu}=3402$, 3048, 2935, 2856, 1668, 1557 cm^{-1}; MS (ESI-TOF): m/z (%): 409.4 (100) $[M+2H]^{2+}$.

Compound *m*-3c: This compound was obtained as described above starting from **1c** and isophthaldehyde, and was characterized as the corresponding HCl salt. Yield: 35%; pale-yellow solid; m.p. 230°C (decomp); $[\alpha]_D^{20}=+7.63$ ($c=0.375$ in CH_3OH); ^{1}H NMR (CD_3OD, 500 MHz): $\delta=1.04$–1.16 (m, 24H), 1.37–1.43 (m, 8H), 1.78 (brs, 4H), 2.11 (d, $J=9.7$ Hz, 4H), 2.29–2.36 (m, 4H), 3.57–3.82 (m, 4H), 3.91–4.30 (m, 12H), 7.40–7.61 ppm (m, 8H); ^{13}C NMR (CD_3OD, 125 MHz): $\delta=18.3$, 19.6, 25.4, 31.0, 33.6, 51.3, 54.1, 66.6, 131.0, 132.4, 132.9, 134.6, 168.0 ppm; IR (KBr): $\tilde{\nu}=3387$, 3215, 3055, 1959, 2936, 2856, 1670, 1554 cm^{-1}; MS (ESI): m/z (%): 415.1 (100) $[M+2H]^{2+}$, 746.1 (30) $[M+Na+K]^{2+}$.

Compound 3e: This compound was obtained as described above starting from **1e** and terephthaldehyde, and was characterized as the free amine. Yield: 58%; white solid; m.p. 232–237°C; $[\alpha]_D^{20}=+11.76$ ($c=1.04$ in $CHCl_3/CH_3OH$ 7:3); ^{1}H NMR ($CDCl_3$ with a few drops of CD_3OD, 500 MHz): $\delta=0.81$–0.84 (brt, $J=6.6$ Hz, 24H), 1.22–1.33 (m, 12H), 1.50–1.52 (m, 8H), 1.71 (brs, 4H), 1.97 (d, $J=10.9$ Hz, 2H), 2.08 (d, $J=11.8$ Hz, 2H), 3.05–3.11 (m, 4H), 3.56 (ABq, $\delta_A=3.59$, $\delta_B=3.52$ ppm, $|J_{AB}|=11.5$ Hz, 8H), 3.63–3.68 (m, 4H), 7.11 (s, 6H), 7.22 ppm (s, 2H); ^{13}C NMR ($CDCl_3$ with drops of CD_3OD, 75 MHz): $\delta=22.5$, 22.8, 24.8, 25.2, 32.7, 42.6, 52.6, 52.9, 61.0, 129.1, 137.8, 175.2 ppm; IR (KBr): $\tilde{\nu}=3302$, 3054, 2932, 2867, 1643, 1516 cm^{-1}; MS (ESI-TOF): m/z (%): 885.6 (100) $[M+H]^+$, 908.7 (95) $[M+Na]^+$, 454.3 (45) $[M+H+Na]^{2+}$.

Compound 3f: This compound was obtained as described above starting from **1f** and terephthaldehyde, and was characterized as the free amine. Yield: 41%; white solid; m.p. 290°C (decomp); $[\alpha]_D^{20}=+17.68$ ($c=0.90$ in $CHCl_3/CH_3OH$ 7:3); ^{1}H NMR ($CDCl_3$, CD_3OD, 500 MHz): $\delta=0.75$ (t, $J=7.3$ Hz, 12H), 0.78 (d, $J=6.8$ Hz, 12H), 0.91–1.01 (m, 4H), 1.13–1.27 (m, 8H), 1.34–1.42 (m, 4H), 1.60–1.66 (m, 8H), 2.02 (d, $J=12.5$ Hz, 4H), 2.84 (brs, 4H), 3.23–3.27 (m, 4H, overlapped with solvent signal), 3.37 (ABq, $\delta_A=3.44$, $\delta_B=3.30$ ppm, $|J_{AB}|=11.6$ Hz, 8H), 3.60–3.62 (m, 4H), 6.95 ppm (s, 8H); ^{13}C NMR ($CDCl_3$, CD_3OD, 75 MHz): $\delta=11.5$, 15.1, 24.4, 25.5, 32.5, 37.7, 52.4, 52.6, 66.7, 128.7, 137.2, 173.7 ppm; IR (KBr): $\tilde{\nu}=3294$, 3056, 3011, 2933, 2857, 1655, 1522 cm^{-1}; MS (ESI-TOF): m/z (%): 885.6 (100) $[M+H]^+$, 907.6 (70) $[M+Na]^+$, 443.3 (65) $[M+2H]^{2+}$, 454.8 (50) $[M+H+Na]^{2+}$.

Compound 3g: This compound was obtained as described above starting from **1g** and terephthaldehyde. To avoid deprotection of the side-chain the reduction was hydrolyzed with a 1 M aqueous solution of ammonium acetate. Yield: 17%; white solid; m.p. 173–178°C; $[\alpha]_D^{20}=+4.06$ ($c=1.20$ in $CHCl_3$); ^{1}H NMR (CD_3OD, 500 MHz): $\delta=1.23$–1.38 (m, 12H), 1.66–1.75 (m, 8H), 1.78–1.85 (m, 4H), 2.03 (d, $J=11.5$ Hz, 4H), 2.25–2.32 (m, 4H), 2.35–2.41 (m, 4H), 3.04 (t, $J=6.6$ Hz, 4H), 3.42 (ABq, $\delta_A=3.52$, $\delta_B=3.32$ ppm, $|J_{AB}|=14.6$ Hz, 8H), 3.65–3.67 (m, 4H), 7.02 (s, 8H), 7.17–7.24 ppm (m, 60H); ^{13}C NMR (CD_3OD, 125 MHz): $\delta=24.6$, 29.4, 32.4, 32.9, 52.0, 52.6, 61.5, 70.4, 126.6, 127.5, 128.5, 128.8, 138.3, 144.8, 173.3, 175.2 ppm; IR (KBr): $\tilde{\nu}=3315$, 3057, 2931, 2857, 1803, 1513 cm^{-1}; MS (ESI-TOF): m/z (%): 639.0 (100) $[M+3H]^{3+}$, 957.9 (90) $[M+2H]^{2+}$.

Compound 5a: Bis(amidoamine) **1c** (50.5 mg, 0.1616 mmol) was dissolved in degassed CH_3OH (3 mL) and the solution was placed inside a flask under nitrogen. Freshly distilled benzaldehyde (33 μL, 0.3232 mmol) was dissolved in degassed CH_3OH (200 μL) and this solution was added to the solution of **1c** (a final concentration of **1c** of 0.05 M). The mixture was stirred overnight and the solvent evaporated in vacuum. The compound obtained showed high purity by NMR and was used without further purification. Yield: quantitative; white solid; m.p. 172–176°C; $[\alpha]_D^{20}=-25.57$ ($c=1.08$ in $CHCl_3$); ^{1}H NMR ($CDCl_3$): $\delta=0.91$ (d, $J=6.8$ Hz, 6H), 0.94 (d, $J=6.8$ Hz, 6H), 1.11–1.19 (m, 2H), 1.26–1.33 (m, 2H), 1.66–1.67 (m, 2H), 2.12 (brs, 1H), 2.15 (brs, 1H), 2.31–2.38 (m, 2H), 3.56 (d, $J=5.0$ Hz, 2H), 3.71–3.75 (m, 2H), 6.99 (brd, $J=6.1$ Hz, 2H), 7.43–7.47 (m, 6H), 7.81 (dd, $J_1=7.2$, $J_2=2.3$ Hz, 4H), 8.14 ppm (s, 2H); ^{13}C NMR ($CDCl_3$, 125 MHz): $\delta=18.4$, 20.0, 24.8, 32.6, 32.8, 53.2, 80.1, 128.8, 128.9, 131.3, 135.9, 162.3, 173.3 ppm; IR (KBr): $\tilde{\nu}=3280$, 3062, 2959, 2931, 2856, 1643, 1533 cm^{-1}; MS (ESI-TOF): m/z (%): 489.3 (100) $[M+H]^+$, 511.3 (90) $[M+Na]^+$.

Compound 5b: This compound was obtained as described above starting from **1h** and benzaldehyde, but the mixture was stirred at RT for 3 d. Yield: 93%; white solid; m.p. 149–155°C; $[\alpha]_D^{20} = -126.21$ ($c = 0.93$ in $CHCl_3$/MeOH 9:1); ^{1}H NMR ($CDCl_3$): $\delta = 0.77$ (d, $J = 6.9$ Hz, 6H), 0.83 (d, $J = 6.9$ Hz, 6H), 1.27–1.42 (m, 4H), 1.74–1.76 (m, 2H), 2.09–2.14 (m, 2H), 2.17 (brs, 1H), 2.19 (brs, 1H), 3.14 (d, $J = 4.6$ Hz, 2H), 3.70–3.75 (m, 2H), 6.81 (brd, $J = 5.7$ Hz, 2H), 7.44–7.46 (m, 6H), 7.56 (s, 2H), 7.64–7.66 ppm (m, 4H); ^{13}C NMR ($CDCl_3$, 125 MHz): $\delta = 17.7$, 19.5, 25.0, 32.8, 32.9, 52.9, 79.6, 128.8, 128.8, 131.3, 135.7, 161.8, 172.9 ppm; IR (KBr): $\tilde{\nu} = 3305$, 3063, 2960, 2933, 2859, 1645, 1537 cm^{-1}; MS (ESI-TOF): m/z (%): 489.23 (100) $[M+H]^+$, 511.24 (50) $[M+Na]^+$.

Compound 5c: This compound was obtained as described above starting from **1a** and benzaldehyde. Yield: quantitative; white solid; m.p. 124–129°C; $[\alpha]_D^{20} = +82.45$ ($c = 1.05$ in $CHCl_3$); ^{1}H NMR ($CDCl_3$): $\delta = 0.89$ (d, $J = 6.8$ Hz, 6H), 0.94 (d, $J = 6.8$ Hz, 6H), 2.30–2.36 (m, 2H), 3.39–3.46 (m, 2H), 3.48–3.55 (m, 2H), 3.58 (d, $J = 3.9$ Hz, 2H), 7.11 (brs, 2H), 7.42–7.47 (m, 6H), 7.77 (d, $J = 6.6$ Hz, 4H), 8.06 ppm (s, 2H); ^{13}C NMR ($CDCl_3$, 125 MHz): $\delta = 17.6$, 19.8, 33.1, 39.3,79.2, 128.7, 128.9, 131.4, 135.7, 162.5, 173.6 ppm; IR (KBr): $\tilde{\nu} = 3378$, 3341, 2963, 2930, 2867, 2846, 2819, 1651, 1519 cm^{-1}; MS (ESI-TOF): m/z (%): 457.22 (100) $[M+Na]^+$, 435.28 (80) $[M+H]^+$, 473.25 (50) $[M+K]^+$.

Compound 5d: This compound was obtained as described above starting from the D,D enantiomer of **1a** and benzaldehyde. It showed spectroscopic data identical to **5c**, as expected for enantiomers. Yield: quantitative; white solid; m.p. 132–136°C; $[\alpha]_D^{20} = -91.39$ ($c = 0.99$ in $CHCl_3$).

Acknowledgements

Dr. Cristian Vicent (SCIC-UJI) is gratefully acknowledged for his helpful assistance with the ESI-TOF mass spectra. This work was supported by the Spanish Ministerio de Educación y Ciencia (CTQ2006-15672-C05-02), CSIC-I3 (200780I001) and Bancaixa-UJI (P11B2004-38). M.B. also thanks the MEC for personal financial support (Formación de Profesorado Universitario, F.P.U.).

[1] For some recent examples, see: a) S. E. Gibson, C. Lecci, *Angew. Chem.* **2006**, *118*, 1392–1405; *Angew. Chem. Int. Ed.* **2006**, *45*, 1364–1377; b) L. A. Wessjohann, B. Voigt, D. G. Rivera, *Angew. Chem.* **2005**, *117*, 4863–4868; *Angew. Chem. Int. Ed.* **2005**, *44*, 4785–4790.

[2] For some examples of related systems, see: a) K. Choi, A. D. Hamilton, *Coord. Chem. Rev.* **2003**, *240*, 101–110; b) K. Choi, A. D. Hamilton, *J. Am. Chem. Soc.* **2003**, *125*, 10241–10249; c) K. Choi, A. D. Hamilton, *J. Am. Chem. Soc.* **2001**, *123*, 2456–2457; d) L. Somogyi, G. Haberhauer, J. Rebek, Jr., *Tetrahedron* **2001**, *57*, 1699–1708; e) M. M. Conn, J. Rebek, Jr., *Chem. Rev.* **1997**, *97*, 1647–1668.

[3] a) L. Gentilucci, A. Tolomelli, F. Squassabia, *Curr. Med. Chem.* **2006**, *13*, 2449–2466; b) C. T. Walsh, *Science* **2004**, *303*, 1805–1810; c) W. A. Loughlin, J. D. A. Tyndall, M. P. Glenn, D. P. Fairlie, *Chem. Rev.* **2004**, *104*, 6085–6117; d) R. C. Reid, L. K. Pattenden, J. D. A. Tyndall, J. L. Martin, T. Walsh, D. P. Fairlie, *J. Med. Chem.* **2004**, *47*, 1641–1651; e) R. C. Reid, G. Abbenante, S. M. Taylor, D. P. Fairlie, *J. Org. Chem.* **2003**, *68*, 4464–4471; f) X. Hu, K. T. Nguyen, C. L. M. J. Verlinde, W. G. J. Hol, D. Pei, *J. Med. Chem.* **2003**, *46*, 3771–3774; g) S. Fernández-López, H.-S. Kim, E. C. Choi, M. Delgado, J. R. Granja, A. Khasanov, K. Kraehenbuehl, G. Long, D. A. Weinberger, K. M. Wilcoxen, M. R. Ghadiri, *Nature* **2001**, *412*, 452–455; h) D. P. Fairlie, G. Abbenante, D. R. March, *Curr. Med. Chem.* **1995**, *2*, 654–686.

[4] a) R. J. Brea, L. Castedo, J. R. Granja, *Chem. Commun.* **2007**, 3267–3269; b) N. Ashkenasy, S. W. Horn, M. R. Ghadiri, *Small* **2006**, *2*, 99–102; c) W. S. Horne, C. D. Stout, M. R. Ghadiri, *J. Am. Chem. Soc.* **2003**, *125*, 9372–9376; d) D. T. Bong, T. D. Clark, J. R. Granja, M. R. Ghadiri, *Angew. Chem.* **2001**, *113*, 1016–1041; *Angew. Chem. Int. Ed.* **2001**, *40*, 988–1011; e) D. Ranganthan, *Acc. Chem. Res.* **2001**, *34*, 919–930.

[5] a) K. Gloe *Macrocyclic Chemistry: Current Trends and Future Perspectives*, Springer, Dordrecht, **2005**; b) D. Parker, *Macrocycle Synthesis: A Practical Approach*, Oxford University Press, New York, **1996**; c) B. Dietrich, P. Viout, J.-M. Lehn, *Macrocyclic Chemistry*, VCH, Weinheim, **1993**; d) F. Vögtle, *Cyclophane Chemistry*, Wiley, Chichester, **1993**; e) N. Sokolenko, G. Abbenante, M. J. Scanlon, A. Jones, L. R. Gahan, G. R. Hanson, D. P. Fairlie, *J. Am. Chem. Soc.* **1999**, *121*, 2603–2604.

[6] a) S. B. Y. Shin, B. Yoo, L. J. Todaro, K Kirshenbaum, *J. Am. Chem. Soc.* **2007**, *129*, 3218–3225; b) D. G. Rivera, L. A. Wessjohann, *J. Am. Chem. Soc.* **2006**, *128*, 7122–7123; c) H. Jiang, J.-M. Léger, P. Guionneau, I. Huc, *Org. Lett.* **2004**, *6*, 2985–2988; d) T. Velasco-Torrijos, P. V. Murphy, *Org. Lett.* **2004**, *6*, 3961–3964; e) T. V. R. S. Sastry, B. Banerji, S. K. Kumar, A. C. Kunwar, J. Das, J. P. Nandy, J. Iqbal, *Tetrahedron Lett.* **2002**, *43*, 7621–7625.

[7] a) M. Amorín, L. Castedo, J. R. Granja, *Chem. Eur. J.* **2008**, *14*, 2100–2111; b) M. Sastry, C. Brown, G. Wagner, T. D. Clark, *J. Am. Chem. Soc.* **2006**, *128*, 10650–10651; c) Z.-T. Li, J.-L. Hou, C. Li, H.-P. Yi, *Chem. Asian J.* **2006**, *1*, 766–778; d) R. P. Cheng, *Curr. Opin. Struct. Biol.* **2004**, *14*, 512–520.

[8] a) N. Delsuc, J.-M. Léger, S. Massip, I. Huc, *Angew. Chem.* **2007**, *119*, 218–221; *Angew. Chem. Int. Ed.* **2007**, *46*, 214–217; b) R. Gray, J. O. Trent, *Biochemistry* **2005**, *44*, 2469–2477; c) M. Jourdan, M. S. Searle, *Biochemistry* **2001**, *40*, 10317–10325.

[9] a) P. Cintas, *Angew. Chem.* **2002**, *114*, 1187–1193; *Angew. Chem. Int. Ed.* **2002**, *41*, 1139–1145; b) J. L. Bada, *Nature* **1995**, *374*, 594–595; c) W. A. Bonner, *Origins Life Evol. Biosphere* **1991**, *21*, 59–111.

[10] a) W. C. Pomerantz, V. M. Yuwono, C. L. Pizzey, J. D. Hartgerink, N. L. Abbot, S. H. Gellman, *Angew. Chem.* **2008**, *120*, 1261–1264; *Angew. Chem. Int. Ed.* **2008**, *47*, 1241–1244; b) W. S. Horne, J. L. Price, J. L. Keck, S. H. Gellman, *J. Am. Chem. Soc.* **2007**, *129*, 4178–4180; c) T. A. Martinek, A. Hetényi, L. Fülöp, I. M. Mádity, G. K. Tóth, I. Dékány, F. Fülöp, *Angew. Chem.* **2006**, *118*, 2456–2460; *Angew. Chem. Int. Ed.* **2006**, *45*, 2396–2400; d) C. Tomasini, G. Luppi, M. Monari, *J. Am. Chem. Soc.* **2006**, *128*, 2410–2420; e) A. I. Jiménez, G. Ballano, C. Cativiela, *Angew. Chem.* **2005**, *117*, 400–403; *Angew. Chem. Int. Ed.* **2005**, *44*, 396–399; f) C. Dolain, H. Jiang, J.-M. Léger, P. Guinneau, I. Huc, *J. Am. Chem. Soc.* **2005**, *127*, 12943–12951; g) D. Yang, J. Qu, W. Li, D.-P. Wang, Y. Ren, Y.-D. Wu, *J. Am. Chem. Soc.* **2003**, *125*, 14452–14457; h) A. I. Jiménez, C. Cativiela, J. Gómez-Catalán, J. J. Pérez, A. Aubry, M. París, M. Marraud, *J. Am. Chem. Soc.* **2000**, *122*, 5811–5821.

[11] For some reviews on foldamers, see: a) M. T. Stone, J. M. Heemstra, J. S. Moore, *Acc. Chem. Res.* **2006**, *39*, 11–20; b) G. Licini, L. J. Prins, P. Scrimin, *Eur. J. Org. Chem.* **2005**, 969–977; c) I. Huc, *Eur. J. Org. Chem.* **2004**, 17–29; d) R. P. Cheng, S. H. Gellman, W. F. DeGrado, *Chem. Rev.* **2001**, *101*, 3219–3232; e) D. J. Hill, M. J. Mio, R. B. Prince, T. S. Hughes, J. S. Moore, *Chem. Rev.* **2001**, *101*, 3893–4011; f) M. S. Cubberley, B. L. Iverson, *Curr. Opin. Chem. Biol.* **2001**, *5*, 650–653; g) S. H. Gellman, *Acc. Chem. Res.* **1998**, *31*, 173–180; h) D. Seebach, J. L. Matthews, *Chem. Commun.* **1997**, 2015–2022.

[12] For a recent review, see: J. Blankenstein, J. Zhu, *Eur. J. Org. Chem.* **2005**, 1949–1964.

[13] a) J. M. Holub, H. J. Jang, K. Kirshenbaum, *Org. Lett.* **2007**, *9*, 3275–3278; b) F. Campbell, J. Plante, C. Carruthers, M. J. Hardie, T. J. Prior, A. J. Wilson, *Chem. Commun.* **2007**, 2240–2242; c) X. Bu, X. Wu, N. L. J. Ng, C. K. Mak, C. Qin, Z. Guo, *J. Org. Chem.* **2004**, *69*, 2681–2685; d) W. Jiang, J. Wanner, R. J. Lee, P. Y. Bounaud, D. L. Boger, *J. Am. Chem. Soc.* **2003**, *125*, 1877–1887; e) X. Bu, X. Wu, G. Xie, Z. Guo, *Org. Lett.* **2002**, *4*, 2893–2895; f) T. D. Clark, M. R. Ghadiri, *J. Am. Chem. Soc.* **1995**, *117*, 12364–12365.

[14] a) W. T. Gong, K. Hiratani, T. Oba, S. Ito, *Tetrahedron Lett.* **2007**, *48*, 3073–3076; b) A. Zhang, Y. Han, K. Yamato, X. C. Zeng, B. Gong, *Org. Lett.* **2006**, *8*, 803–806; c) C. Rotger, M. N. Pina, M. Vega, P. Ballester, P. M. Deya, A. Costa, *Angew. Chem.* **2006**, *118*, 6998–7002; *Angew. Chem. Int. Ed.* **2006**, *45*, 6844–6848; d) L. Yuan, W. Feng, K. Yamato, A. R. Sanford, D. Xu, H. Guo, B. Gong, *J. Am.*

Chem. Soc. **2004**, *126*, 11120–11121; e) M. C. Rotger, M. N. Pina, A. Frontera, G. Martorell, P. Ballester, P. M. Deya, A. Costa, *J. Org. Chem.* **2004**, *69*, 2302–2308; f) F. J. Carver, C. A. Hunter, R. J. Shannon, *J. Chem. Soc., Chem. Commun.* **1994**, 1277–1280.

[15] a) C. Peña, I. Alfonso, V. Gotor, *Eur. J. Org. Chem.* **2006**, 3887–3897; b) J. E. W. Scheuermann, K. F. Sibbons, D. M. Benoit, M. Motevalli, M. Watkinson, *Org. Biomol. Chem.* **2004**, *2*, 2664–2670; c) G. Stones, G. Argouarch, A. R. Kennedy, D. C. Sherrington, C. L. Gibson, *Org. Biomol. Chem.* **2003**, *1*, 2357–2363; d) B. Altava, M. I. Burguete, B. Escuder, S. V. Luis, E. García-España, M. C. Muñoz, *Tetrahedron* **1997**, *53*, 2629–2640; e) J. E. Richman, T. J. Atkins, *J. Am. Chem. Soc.* **1974**, *96*, 2268–2270.

[16] a) D. Zhao, J. S. Moore, *J. Org. Chem.* **2002**, *67*, 3548–3554; b) R. A. Abramovitch, X. Ye, W. T. Pennington, G. Schimek, D. Bogdal, *J. Org. Chem.* **2000**, *65*, 343–351; c) R. A. Abramovitch, X. Ye, *J. Org. Chem.* **1999**, *64*, 5904–5912.

[17] A. Saghatelian, Y. Yokobayashi, K. Soltani, M. R. Ghadiri, *Nature* **2001**, *409*, 797–801.

[18] J. Becerril, M. Bolte, M. I. Burguete, F. Galindo, E. García-España, S. V. Luis, J. F. Miravet, *J. Am. Chem. Soc.* **2003**, *125*, 6677–6686.

[19] a) J. Becerril, B. Escuder, J. F. Miravet, R. Gavara, S. V. Luis, *Eur. J. Org. Chem.* **2005**, 481–485; b) J. Becerril, M. I. Burguete, B. Escuder, F. Galindo, R. Gavara, J. F. Miravet, S. V. Luis, G. Peris, *Chem. Eur. J.* **2004**, *10*, 3879–3890; c) J. Becerril, M. I. Burguete, B. Escuder, S. V. Luis, J. F. Miravet, M. Querol, *Chem. Commun.* **2002**, 738–739.

[20] I. Alfonso, M. I. Burguete, S. V. Luis, J. F. Miravet, P. Seliger, E. Tomal, *Org. Biomol. Chem.* **2006**, *4*, 853–859.

[21] a) M. I. Burguete, F. Galindo, M. A. Izquierdo, S. V. Luis, L. Vigara, *Tetrahedron* **2007**, *63*, 9493–9501; b) M. I. Burguete, F. Galindo, S. V. Luis, L. Vigara, *Dalton Trans.* **2007**, 4027–4033; c) F. Galindo, M. I. Burguete, L. Vigara, S. V. Luis, D. A. Russell, N. Kabir, J. Gavrilovic, *Angew. Chem.* **2005**, *117*, 6662–6666; *Angew. Chem. Int. Ed.* **2005**, *44*, 6504–6508; d) F. Galindo, J. Becerril, M. I. Burguete, S. V. Luis, L. Vigara, *Tetrahedron Lett.* **2004**, *45*, 1659–1662.

[22] a) I. Alfonso, M. I. Burguete, F. Galindo, S. V. Luis, L. Vigara, *J. Org. Chem.* **2007**, *72*, 7947–7956; b) I. Alfonso, M. I. Burguete, S. V. Luis, *J. Org. Chem.* **2006**, *71*, 2242–2250.

[23] N. E. Borisova, M. D. Reshetova, Y. A. Ustynyuk, *Chem. Rev.* **2007**, *107*, 46–79.

[24] a) I. Alfonso, M. Bolte, M. Bru, M. I. Burguete, S. V. Luis, J. Rubio, *J. Am. Chem. Soc.* **2008**, *130*, 6137–6144; b) M. Bru, I. Alfonso, M. I. Burguete, S. V. Luis, *Angew. Chem.* **2006**, *118*, 6301–6305; *Angew. Chem. Int. Ed.* **2006**, *45*, 6155–6159.

[25] M. Bru, I. Alfonso, M. I. Burguete, S. V. Luis, *Tetrahedron Lett.* **2005**, *46*, 7781–7785.

[26] a) J. Gawroñski, M. Kwit, J. Grajewski, J. Gajewy, A. Dlugokinska, *Tetrahedron: Asymmetry* **2007**, *18*, 2632–2637; b) M. Kwit, A. Plutecka, U. Rychlewska, J. Gawroñski, A. F. Khlebnikov, S. I. Kozhushkov, K. Rauch, A. De Meijere, *Chem. Eur. J.* **2007**, *13*, 8688–8695; c) J. Gawroñski, K. Gawronska, J. Grajewski, M. Kwit, A. Plutecka, U. Rychlewska, *Chem. Eur. J.* **2006**, *12*, 1807–1817; d) N. Kuhnert, A. M. Lopez-Periago, G. M. Rossignolo, *Org. Biomol. Chem.* **2005**, *3*, 524–537; e) N. Kuhnert, N. Burzlaff, C. Patel, A. Lopez-Periago, *Org. Biomol. Chem.* **2005**, *3*, 1911–1921; f) J. Gawroñski, M. Brzostowska, M. Kwit, A. Plutecka, U. Rychlewska, *J. Org. Chem.* **2005**, *70*, 10147–10150; g) N. Kuhnert, G. M. Rossignolo, A. M. Lopez-Periago, *Org. Biomol. Chem.* **2003**, *1*, 1157–1170; h) N. Kuhnert, C. Straßnig, A. M. Lopez-Periago, *Tetrahedron: Asymmetry* **2002**, *13*, 123–128; i) M. Chadim, M. Budì insky, J. Hodaèova, J. Zavada, P. C. Junk, *Tetrahedron: Asymmetry* **2001**, *12*, 127–133; j) J. Gawroñski, H. Kołbon, M. Kwit, A. Katrusiak, *J. Org. Chem.* **2000**, *65*, 5768–5773.

[27] a) A. González-Álvaarez, I. Alfonso, V. Gotor, *Chem. Commun.* **2006**, 224–226; b) A. González-Álvarez, I. Alfonso, F. López-Ortiz, A. Aguirre, S. García-Granda, V. Gotor, *Eur. J. Org. Chem.* **2004**, 1117–1127.

[28] a) S. Hanessian, V. Vinci, K. Fettis, T. Maris, M. T. P. Viet, *J. Org. Chem.* **2008**, *73*, 1181–1191; b) C. Peña, I. Alfonso, B. Tooth, N. H. Voelcker, V. G. Gotor, *J. Org. Chem.* **2007**, *72*, 1924–1930.

[29] a) N. Berova, L. Di Bari, G. Pescitelli, *Chem. Soc. Rev.* **2007**, *36*, 914–931; b) N. Berova, K. Nakanishi, R. W. Woody, *Circular Dichroism. Principles and Applications*, Wiley-VCH, New York, **2000**.

[30] M. Kaik, J. Gawroñski, *Org. Lett.* **2006**, *8*, 2921–2924.

[31] Experimental support for this hypothesis can be obtained from the NMR spectroscopy data obtained for **1c** and **1h** in $CDCl_3$ (see the Supporting Information). The chemical shifts of the amide NH protons are $\delta = 7.25$ and 7.36 ppm for **1c** and **1h**, respectively. This suggests the proton in **1h** has a greater hydrogen-bonded character. We thank the suggestion of an anonymous referee who prompted us to revise these data.

[32] a) N. J. Greenfield, *Anal. Biochem.* **1996**, *235*, 1–10; b) A. Percze1, M. Hollósi, B. M. Foxman, G. D. Fasman, *J. Am. Chem. Soc.* **1991**, *113*, 9772–9782.

[33] L. You, R. Ferdani, R. Li, J. P. Kramer, R. E. K. Winter, G. W. Gokel, *Chem. Eur. J.* **2008**, *14*, 382–396; and references therein.

[34] E. Gouaux, R. MacKinnon, *Science* **2005**, *310*, 1461–1465.

[35] R. H. Blessing, *Acta Crystallogr., Sect. A* **1995**, *51*, 33–38.

[36] G. M. Sheldrick, *Acta Crystallogr., Sect. A* **2008**, *64*, 112–122.

[37] Spartan '06. Wavefunction, Inc., Irvine, CA (USA).

Received: April 15, 2008
Published online: August 7, 2008

